ESRF	**Experiment title:** High-resolution tomography on metal foams in very early expansion stages.	**Experiment number:** ME-293
Beamline: ID19	**Date of experiment:** from: 06/09/01 to: 10/09/01	**Date of report:** 04/09/02
Shifts: 9	**Local contact(s):** E. Boller	*Received at ESRF:*

Names and affiliations of applicants (* indicates experimentalists):
L. Helfen*, T. Baumbach*: Fraunhofer IZFP, Saarbruecken, Germany; J. Banhart, H. Stanzick: Fraunhofer IFAM, Bremen, Germany; P. Pernot*: ESRF, Grenoble

Report:

During ME-41 we investigated the early foaming stages [HBS+02] of aluminium alloy (AlSi7 and AA6061) and zinc foam formation fabricated by the powder metallurgical route. Closer evaluation of the experimental data of ME-41 indicated that for AA6061 there is a high spatial correlation between the TiH_2 particles and evolving pores from the onset of foam expansion. Obviously the bonding strength between alloy powder particles is higher than the bonding strength between alloy particles and blowing agent particles.

For AlSi7, at the beginning of foaming, pores and blowing agent are less correlated and correlation increases during foaming. This arises the question where the pores nucleate for this material. The different fabrication approach based on two powders (instead of one pre-alloy used for AA6061) suggested that pores could nucleate nearby Si particles after diffusion of the hydrogen through the solid metallic matrix.

The aim of this experiment was therefore to examine more closely the very early foaming stages up to approximately 10 percent expansion. In especially we determined the structure of cut-out portions of the most dense samples of the two alloy series already investigated in ME-41.

In Fig. 1 we see 3D renditions of the acquired data sets after tomographic reconstruction. The light spots on the rendered cubes are highly absorbing regions and show the spatial distribution of the blowing agent particles and residual highly absorbing impurities. The pores are rendered transparent and are at the shown expansion stages $\varepsilon = 0.09$ (AlSi7) and $\varepsilon = 0.01$ (AA6061) visible as thin fissures through the metallic matrix which has, during heat treatment, not reached its solidification temperature.

The reason for the higher spatial correlation in the case of AA6061 becomes apparent if one examines reconstructed slices taken with 0.7 μm pixel size, as shown in Fig. 2. In the AlSi7 sample we find sharp-edged regions with a grey level of the alloy matrix. They are, in fact, the silicon powder particles used to fabricate the alloy. The cracks are very often found around these Si particles and not in the surroundings of the blowing agent. When heating up an AlSi7 precursor material stemming from three base powders (Al, Si and blowing agent) the interface between Al and Si will get liquid first since the solidification temperature is reduced to the eutectic temperature. Perharps in this way, pores nucleate first at the Al-Si interface and subsequently cracks are prone to propagate along the Si particles.

In the AA6061 samples the sharp-edged regions described above are not found. They do not have their counterpart in the AA6061 samples as they are produced from a pre-alloyed powder. Almost all blowing agent show pores around them, indicating that pore nucleation takes place locally.

We therefore investigated the most dense AlSi7 sample ($\varepsilon = 0.09$) by means of holographic wavefield reconstruction technique similar to the one presented in [Clo99a, Clo99b]. At an x-ray energy of 18 keV we carried out at four distances $i = 1, \ldots, 4$; $z_i \in [0.004, 0.064, 0.154, 0.4]$ m a tomographic scan with 1400 projection radiographs with a pixel size of 0.7μm.

We treated the experimental data by a method proposed in [Lud01]: in order to eliminate the intensity modulations caused by absorption we divided each intensity pattern of a distance z_i, $i = 2, 3, 4$, by the approximate absorption radiagraph at z_1. From these data we reconstructed by the reconstruction method the projected phase maps $\phi(\vec{x})$ according to [Lud01] and therefrom by filtered backprojection. the refractive index decrement δ. This approach has been shown to work [Lud01] on samples causing a rather smooth amplitude modulation which can be approximated by a smooth envelope. As our AlSi7 sample shows strong amplitude modulations, especially if the beam direction is almost parallel to the thin fissures, we attribute the rather low contrast and artifacts in the reconstructed image (see below) to the approximations which are not satisfied in this case.

Fig. 3 shows corresponding slices of the reconstruced absorption image and of the holographically recon-

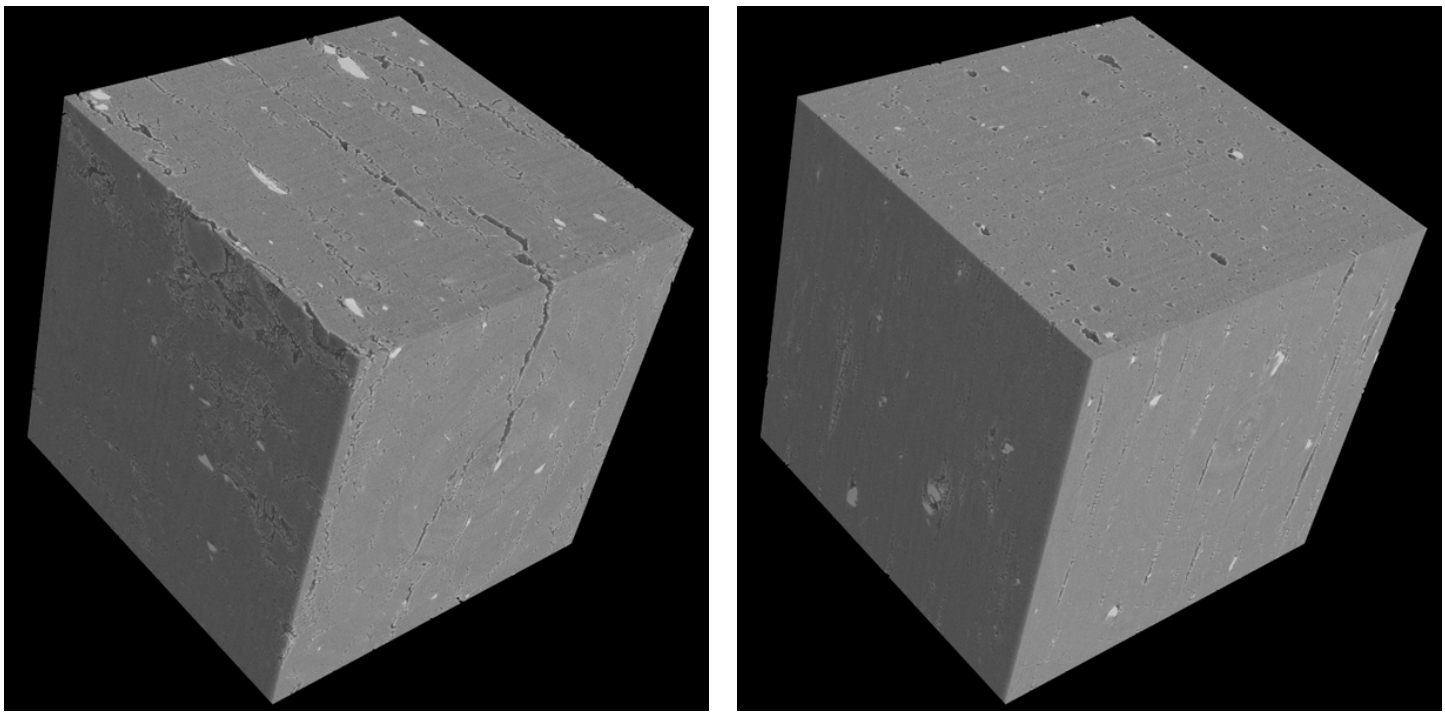

Figure 1: 3D renditions of reconstructed volume data of the two most dense samples of both series: AlSi7 $\varepsilon = 0.09$ (left) and AA6061 $\varepsilon = 0.01$ (right). Volume sizes are $660 \times 660 \times 660$ voxels with a linear dimension of 0.7 μm, translating into a side length of about 0.46 mm for each cube. The light regions stand for a large linear attenuation coefficient μ and correspond to the strongly absorbing blowing agent and residual impurities.

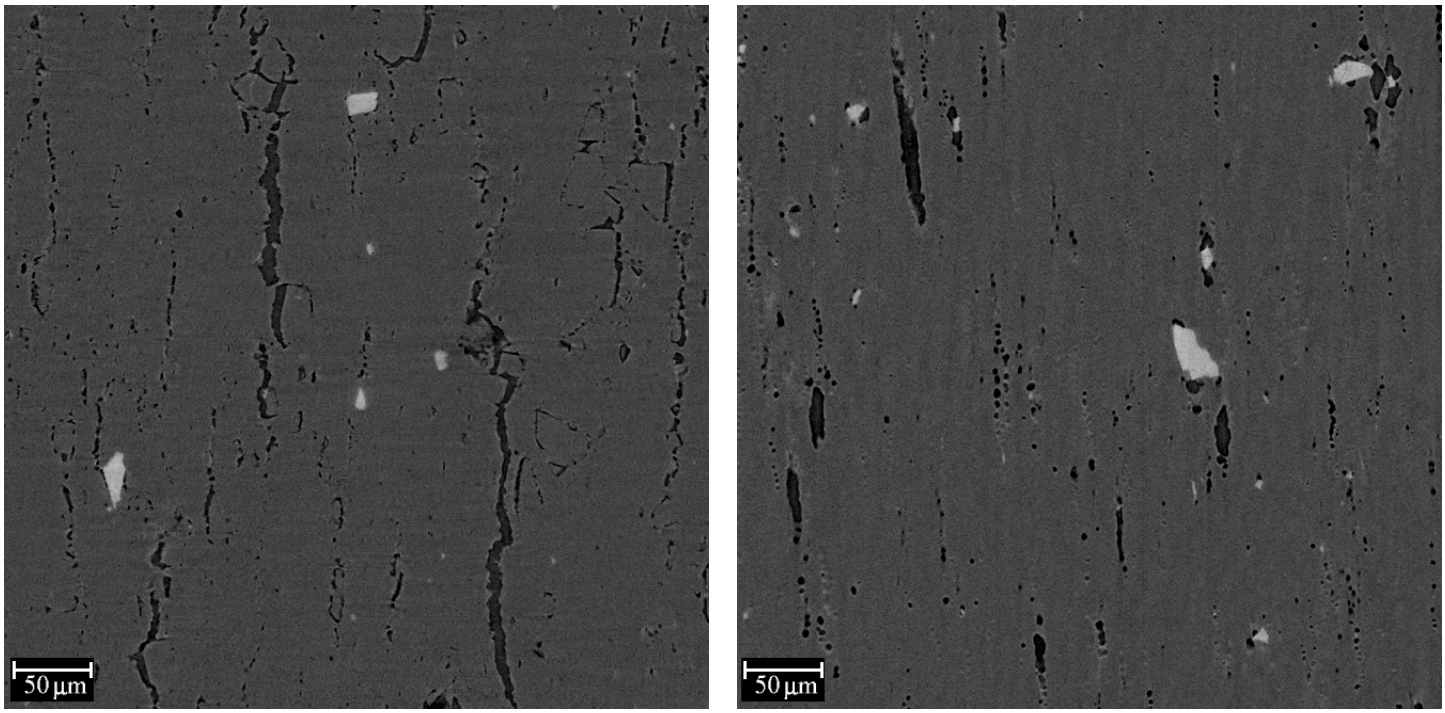

Figure 2: Reconstructed slices of the two most dense samples of both series. Image sizes are 660×660 voxels of $0.7 \times 0.7\,\mu\mathrm{m}^2$ size. The AlSi7 sample (left) exhibits dark grey, sharply edged regions which do not appear in the AA6061 sample (right).

structed image. As usual, the absorption image shows the local linear absorption (which is proportional to the imaginary part of the refractive index), i. e. lowly absorbing regions dark and vice versa. Thus, pores and cracks are shown in this image in black and the remnants of the blowing agent TiH_2 in white. The remaining grey regions are the Al-Si matrix in which Al and Si regions are not distinguishable because of the very similar absorption of the two elements. Moreover, we see that at the border of the matrix towards pores is emphasised slightly by phase contrast.

As opposed to the absorption image the holographic image (bottom image of Fig. 3) shows reversed contrast because of the sign of the refractive index decrement $\delta \propto \rho_e$. Thus, white regions are the pores, black regions the blowing agent TiH_2 with a high electronic density ρ_e. Within the metallic matrix one can see two predominant grey levels, the lighter one corresponding to Si with a higher electronic density, the darker more frequent one to Al with a lower electronic density. The regions corresponding to Si are rather irregularly polyhedral in projection which corresponds in 3D to irregularly edged particles.

From a comparison between the two images we conclude that among the pores visible there are a some of them in direct neighbourhood of a Si particle. Considering the entity of reconstructed data, a significant number of pores is found in such a direct neighbourhood to Si. For example, looking carefully again at Fig. 1 we see that at the surface of the rendered cube there are a number of such edged particles visible. Around these, cracks are spread preferentially perpendicular to the precursor compression axis and they

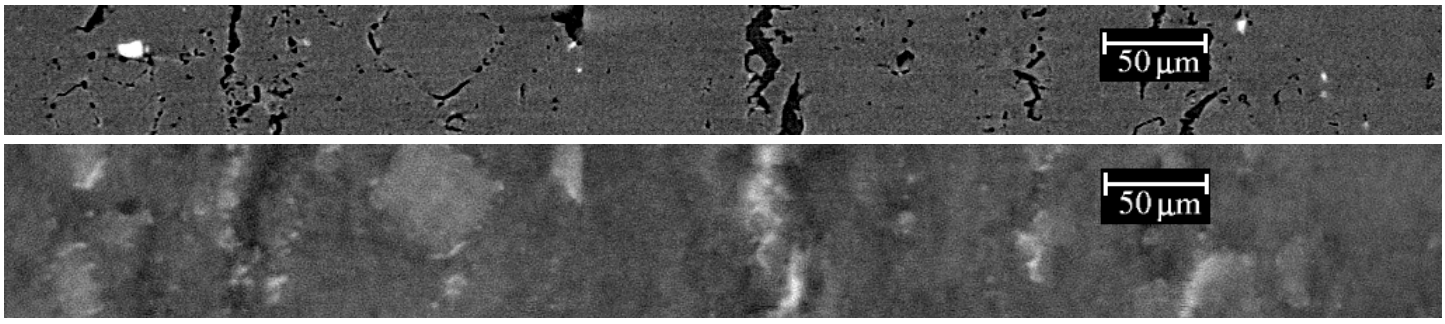

Figure 3: Corresponding reconstructed slices through the most dense AlSi7 foam ($\varepsilon = 0.09$) in absorption mode (top) and holographic mode (bottom). Pixel size is 0.7μm, width 1024 pixels.

are partly connecting these particles.

We conclude that in AlSi7 made from two base powders pores nucleate predominantly at the interface between Al and Si in the metallic matrix. Perhaps in this way, cracks propagate along spatial agglomerations of Si particles and towards the blowing agent particles. Furthermore, melting is supposed to start first at the interface between Al and Si since the two-phase system has a lower solidification temperature than bulk Al.

References

[Clo99a] P. Cloetens. *Contribution to Phase Contrast Imaging, Reconstruction and Tomography with Hard Synchrotron Radiation.* PhD thesis, Vrije Universiteit Brussel, Brussel, Belgium, 1999.

[Clo99b] P. Cloetens. Holotomography: Quantitative phase tomography using coherent synchrotron radiation. *Appl. Phys. Lett.*, 75:2912, 1999.

[HBS+02] L. Helfen, T. Baumbach, H. Stanzick, J. Banhart, A. Elmoutaouakkil, and P. Cloetens. Viewing the early stage of metal foam formation by computed tomography using synchrotron radiation. *Adv. Eng. Mater.*, 4:accepted for publication, 2002.

[Lud01] W. Ludwig. *Development and applications of synchroton radiation microtomography.* PhD thesis, Ludwig-Maximilians-Universität, München, Germany, 2001.